



UNIVERSITY OF NIŠ

The scientific journal FACTA UNIVERSITATIS

Series: Mechanics, Automatic Control and Robotics Vol.2, No 10, 2000 pp. 1299 - 1317

Editor of series: Katica (Stevanovi) Hedrih, e-mail: katica@masfak.masfak.ni.ac.yu

Address: Univerzitetski trg 2, 18000 Niš, YU, Tel: +381 18 547-095, Fax: +381 18 547-950

http://ni.ac.yu/Facta

VISCOPLASTIC BEHAVIOR OF DAMAGED AISI 316H FROM DYNAMIC EXPERIMENTS

UDC 620.17:669.14(045)

M. Mićunović¹, M. Radosavljević², C. Albertini³, M. Montagnani³

¹ Faculty of Mechanical Engineering, Kragujevac, Yugoslavia

E-mail: mmicun@knez.uis.kg.ac.yu

² Higher Technical School, Kragujevac, Yugoslavia

³ JRC CEC, I-21020 Ispra(VA), Italy

Abstract. *The group of specimens, previously subjected either to creep or low cycle fatigue, are examined by tension at 550°C in the strain-rate range $[10^{-3}, 10^3] s^{-1}$. The specimens previously treated by creep suffered various levels of creep strains while the specimens predamaged by LCF had various LCF strain critical cycle numbers (as a measure of initial life time). Evolution equations are calibrated for as-received, creep-damaged and LCF-damaged specimens, covering stress-strain strain-rate relations and accounting for strain and strain-rate hardening. The material constants entering the equations are damage-dependent. Comparisons with some empirical and microstructural models are made.*

Key words: *creep and LCF predamage, viscoplastic experiments, inelastic history, Rabotnov's delay, constitutive modelling, material constants identification*

1 Experimental Evidence and Definition of the Problem

The test material, AISI 316H stainless steel, had been received as a mill-annealed 50 mm thick hot-rolled plate with the following percentually expressed chemical composition:

Cr	Ni	Mn	Mo	Nb	C	Si	S
16.9	12.4	1.65	2.45	0.006	0.053	0.35	0.008

The observed grain size range of the as-received material was $[70, 90] \mu\text{m}$. The predamage treatment was as follows :

- LCF tests were carried out by PNC-Tokyo at the University of Tokyo with the hourglass-shaped specimens using an electro-hydraulic closed loop fatigue test machine under triangular wave shape and strain rate of approximately 0.001 s^{-1} (details are given in [1]). The specimens were heated by an induction heater and the temperature in the test section was maintained in the range $550 \pm 2 [^{\circ}\text{C}]$. The cycle strain amplitude was either 0.6% or 1% with cycle ratios $n/N_F \in \{0.2, 0.4, 0.6\}$ where N_F is ultimate (life) cycle number.
- Creep tests performed at the JRC-Ispra were accomplished also at 550°C with a constant tensile stress of 300 MPa and a creep life time of $T_c = 2000 \text{ h}$. These tests were interrupted at 423 h , 823 h and 1220 h (i.e. approximately at $t/T_c \in \{0.2, 0.4, 0.6\}$ creep life time ratios).

Prior to the actual testing, thin outer layers of the cylindrical specimens, previously subjected either to LCF or creep, were removed in order to exclude surface microcracks. Subsequently, the bulk specimens were split longitudinally by electric discharge machining and the small, final test specimens were machined out from each singular piece. All the mentioned specimens had cylindrical gauge parts (for their geometrical details cf. [9]).

The actual tensile test was carried out in the following three regimes :

- at the lowest strain rate of 0.0035 s^{-1} by an Instron machine;
- at medium strain rates in the range $[10^{-1}, 10^2] \text{ s}^{-1}$ by a hydro-pneumatic machine installed in a hot cell of the Medium Activity Laboratory of the JRC-Ispra and
- at high strain rates in the range $[10^2, 10^3] \text{ s}^{-1}$ by a modified Hopkinson bar with a prestressed loading device installed in a hot cell of the High Activity Laboratory of the JRC-Ispra.

The last two apparatuses had been developed in Ispra and are described in detail in [2]. The test results for the creep tests are presented in Figure 1. for strain rates falling in the range $\{0.0035, 3.5, 750\} \text{ s}^{-1}$. For the sake of clarity, three-dimensional plots are chosen with engineering stress σ , strain ε and relative age time $\tau = t/T_c$ as variables. The various strain rate regimes are given by the mentioned relative age times $\tau \in \{0, 0.2, 0.4, 0.6\}$, respectively.

Concerning low cycle fatigue, in figure 2. the corresponding plots are shown for a previous LCF-strain amplitude $\Delta\varepsilon = 0.6\%$ at strain rates in the range $\{0.0035, 1.5, 550\} \text{ s}^{-1}$, respectively. Apart from stress and strain, the cycle ratio $\nu = n/N_F$ is chosen to represent damage measure as the third variable in the plots. The various strain rate regimes are given by the mentioned cycle ratio $\nu \in \{0, 0.2, 0.4, 0.6\}$, respectively.

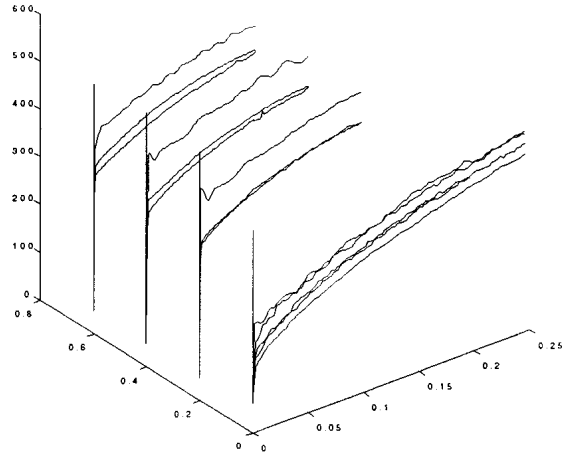


Figure 1: Stress $\sigma(\epsilon_P, \tau)$ for low, medium and high $d\epsilon_P/dt$ at diverse previous creep times

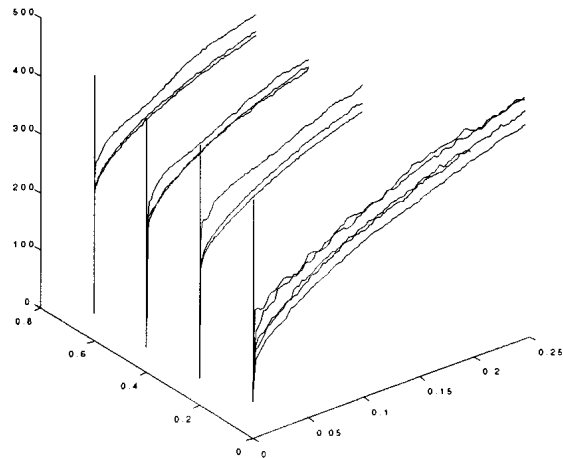


Figure 2: Stress $\sigma(\epsilon_P, \nu)$ for low, medium and high $d\epsilon_P/dt$ at previous LCF with $\Delta\epsilon = 0.6\%$ and diverse cycle ratios

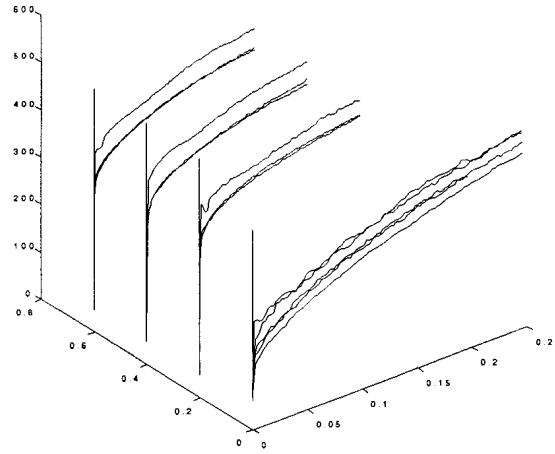


Figure 3: Stress $\sigma(\varepsilon_P, \nu)$ for low, medium and high $d\varepsilon_P/dt$ at previous LCF with $\Delta\varepsilon = 1\%$ and diverse cycle ratios

Finally, Figure 3. is different from Figure 2. only in previous LCF-strain amplitude which now is $\Delta\varepsilon = 1\%$.

As a general tendency, both damage processes provoke, for a fixed strain rate, an increase in the initial yield stress and (not so marked) ultimate tensile stress; a reduction of ductility, represented by the fracture strain; and (more pronounced) uniform strain.

The first phenomenon might be called conditionally a damage hardening while the second, leading to higher sensitivity of damaged materials caused by void accumulation during a damage process, is also important and must be taken into account.

From the figures we observe also that up to large strain values for a fixed strain, there exists strain rate hardening, i.e. an increase of flow (yield) stress with increasing strain rate. Finally, the observed dynamic strain aging serrations are analyzed elsewhere [3] and are not considered in this paper.

If we want to give some analytical expression accounting for the above discussed phenomena, the following simple, yet general, formula seems to be appropriate :

$$\begin{aligned} \text{uniaxial flow stress} = f(\text{strain, strain rate, damage history,} & \quad (1) \\ & \text{plastic strain history, plastic strain rate history}) \end{aligned}$$

If damage is represented by a tensorial variable, say \mathcal{D} (cf. [14]), then the above relationship might be alternatively written by the following functional:

$$\sigma(t) = \mathcal{F}_{\xi=0}^{\infty} [\varepsilon_P(t - \xi), \dot{\varepsilon}_P(t - \xi), \mathcal{D}(t - \xi)], \quad (2)$$

where t is actual time, ξ - time distance to a past time, $\varepsilon_P(t - \xi)$ and $\dot{\varepsilon}_P(t - \xi)$ are past and actual plastic strain and plastic strain rate whereas the actual engineering stress is denoted by $\sigma(t)$.

Obviously, the above relationship is too general for a comparison with experiments. Some simplifications of the above model and their calibration are the subject of the next sections.

2 Some Models with Multiplicative History

The principal question to be answered here is the following:

- Is it possible to propose a unified evolution equation among stress, strain and strain rate with a minimal number of (temperature and history-dependent) material "constants" in such a way that a maximal collection of experimental stress-strain diagrams is described within a beforehand prescribed accuracy?

Such a question is the natural consequence of the law (2) specified to applicability in FEM-codes which do require a unified equation for improving the safety analysis of reactor structures subject to complex thermomechanical processes. The common notion in viscoplasticity is the overstress [4, 5, 6], i.e. the difference between the actual ("dynamic") stress and its static counterpart (at negligible plastic strain rate). According to this concept the following uniaxial functional equation is most naturally accepted:

$$\sigma = \sigma^{\#}(\varepsilon_P, \theta, h) [1 + \Delta(\dot{\varepsilon}_P, \varepsilon_P, \theta, h)] \equiv \sigma^{\#} + \Sigma, \quad (3)$$

where:

- σ is the engineering (first Piola-Kirchhoff) dynamic stress,
- $\sigma^{\#}$ its static counterpart,
- ε_P engineering (Lagrangian) uniaxial plastic strain,
- $\dot{\varepsilon}_P$ its material time derivative,
- θ is the relative temperature

$$\theta \equiv \frac{T - T_{room}}{T_{melting} - T_{room}}$$

T the absolute temperature

h stands for stress-strain history (accounting for previous either creep or LCF-regimes) while

Δ and Σ are, respectively, relative and the absolute overstress:

$$\Delta = \frac{\sigma - \sigma^{\#}}{\sigma^{\#}} \equiv \frac{\Sigma}{\sigma^{\#}}. \quad (4)$$

If we want to calibrate the equation (3), then we see that it is too general. Its possible simplification originating from diverse behaviour of curves depicted on figures 1.-3. might be :

$$\sigma = \sigma^\#(\varepsilon_P, \theta) [1 + \Delta(\dot{\varepsilon}_P, \varepsilon_P, \theta) + \Psi_h(h) \Psi_\varepsilon(\varepsilon_P, \theta)], \quad (5)$$

or, by means of $\Psi_h \Psi_\varepsilon \equiv \Psi$, equivalently:

$$\Psi = \frac{\sigma}{\sigma^\#} - 1 - \Delta. \quad (6)$$

Virgin or "as-received" specimens are distinguished by means of so-called zero-history i.e. $\Psi = 0$, whereas static flow stress for $\Delta = 0$ has a multiplicative history modification $\sigma^\#(1+\Psi)$. For this reason, the proposal (5) could be termed as *multiplicative history* evolution equation.

In the sequel some of commonly accepted constitutive models modified by means of multiplicative history are considered. Let us start from the simplest of them. Since all the available experimental data are acquired only at the temperature of 550°C temperature dependence will be omitted unless it is explicitly required by the constitutive model considered.

2.1 Johnson-Cook model

In this model the static stress is modelled by means of the formula:

$$\sigma^\# = Y^\#(1 + C_1 \varepsilon_P^{C_2})(1 - \theta^n) \equiv Y(1 + C_1 \varepsilon_P^{C_2}) \quad (7)$$

and the relative overstress is accounted in a very simple manner [8]:

$$\Delta = C_3 \ln \left[\frac{\dot{\varepsilon}_P}{C_4} \right], \quad (8)$$

where $C_4 \equiv \dot{\varepsilon}_{P \min}$ is a "static" strain rate (i.e. the smallest strain rate of the strain-rate range considered) and C_3 is a constant giving rise to a invariable strain-rate hardening. The model is determined by six material constants: $Y^\#, C_1, \dots, C_4$ and n . Alternatively, when all testing program is at a single temperature, constants to be determined would be Y, C_1, \dots, C_4 .

2.2 Ludwik-Prandtl model

For this model the static stress derived essentially from the Ramberg-Osgood law may be given by the following slight (but essentially non-linear) modification of Ludwik-Hollomon-Swift empirical equation (see also [7]):

$$\sigma^\# = Y(\theta) \left[1 + L_1(\theta) \varepsilon_P^{L_2(\theta)} \right] \quad (9)$$

where Y is the initial yield stress. For the relative overstress coefficient we have at our disposal the Ludwik-Prandtl equation

$$\Delta = a(\theta) \ln \left[\frac{\dot{\varepsilon}_P}{b(\theta)} \right]$$

Comparing the overstress proposed by Johnson and Cook with this formula we see that in the original Ludwik-Prandtl formula they just made only specialization $a(\theta) \equiv C_3$ and $b(\theta) \equiv C_4$ neglecting temperature dependence of these material constants. Its generalization which takes into account temperature as well as strain sensitivity in strain rate hardening i.e.:

$$\Delta = L_3(\theta) \exp[-L_5(\theta)\varepsilon_P] \ln \left[\frac{\dot{\varepsilon}_P}{L_4(\theta)} \right] \quad (10)$$

seems reasonable for description of our experimental data. Again, L_4 is the minimal plastic strain rate corresponding to vanishing of the relative overstress (“control” strain rate in the terminology of [4]).

2.3 Zener-Hollomon model

Let us accept a constitutive equation for the static stress in the form (9). In this model the relative overstress is represented by means of the following formula:

$$\Delta = \left[1 + \frac{\dot{\varepsilon}_P}{c(\theta)} \right]^{d(\theta)} - 1.$$

Again, a generalization similar to (10)

$$\Delta = H_3(\theta) \exp[-H_5(\theta)\varepsilon_P] \dot{\varepsilon}_P^{H_4(\theta)} \quad (11)$$

is going to be checked here. However, meaning of strain rate hardening exponent H_4 must not be confused with L_4 since here this constant has not the meaning of the control strain rate. Vanishing of the relative overstress here appears when $\dot{\varepsilon}_P \rightarrow 0$.

2.4 Armstrong-Zerilli model

In their paper [12] based on dislocation mechanics, Zerilli and Armstrong derived for body centre cubic (bcc) metals the following evolution uniaxial equation:

$$\Sigma = d_1 \exp(-d_3 T) \dot{\varepsilon}_P^{d_4 T} \quad (12)$$

$$\sigma^\# = d_5 + d_6 l^{-1/2} + d_2 \varepsilon_P^{d_7} \quad (13)$$

where T is the absolute temperature and l is the average grain diameter. Collecting both parts into a single evolution equation, we might write:

$$\sigma = Y(\theta) \left[1 + A_1(T) \varepsilon_P^{A_2(T)} + A_3(T) \dot{\varepsilon}_P^{A_4(T)} \right] \quad (14)$$

This collection of material constants has been chosen since in the experiments analyzed in this paper the average grain diameter was not measured. Comparing this equation with the previous two equations (12)-(13) we may write the relations between the two sets of material constants:

$$Y_0 = d_5 + d_6 l^{-1/2}, A_1 = \frac{d_2}{Y_0}, A_2 = d_7, A_3 = \frac{d_1}{Y_0} \exp(-d_3 T), A_4 = d_4 T.$$

which may be solved for various values of plastic strain if the grain diameter is known.

2.5 History quantification

In order to see whether the assumption (6) about multiplicative history is justified, we will quantify Ψ_h and Ψ_ε as follows.

Let us show the procedure for the JC-model. First, we determine Y, C_1, \dots, C_4 for all the tests of as-received specimens. Then we calculate Ψ for fixed histories on three graphs - one for previous creep and the other two for previous LCF with $\Delta\varepsilon = 0.6\%$ and $\Delta\varepsilon = 1\%$ respectively. One of these graphs is depicted on the figure 4. On each of its $\tau = const$ subplots the first tooth-like subsubplot is responsible for low, the second for medium and the third for high strain rate, respectively. The abscissa of the each subsubplot consists of temporal points and since, roughly speaking, plastic strain is proportional to time at each subsubplot we may note an exponential decay of Ψ_ε with ε_P .

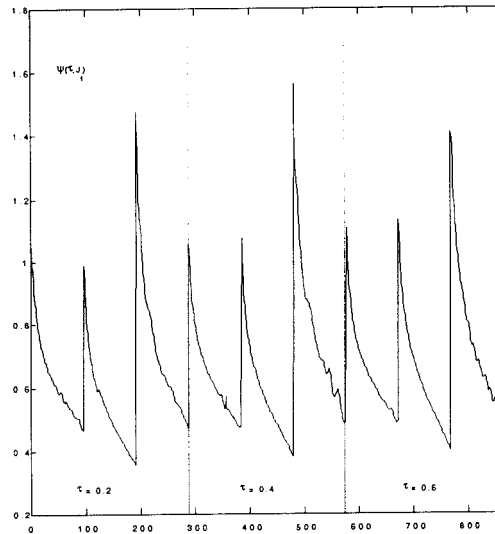


Figure 4: Multiplicative history Ψ versus temporal index J_i for previous creep

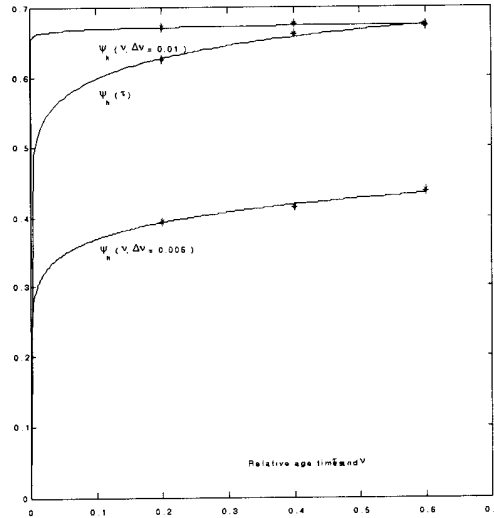


Figure 5: Damage hardening history functions

Let us now quantify the constituent Ψ_h in the damage history. To do this, we find average values of Ψ for each subplot (i.e. for $\tau = 0.2, \dots, v(\Delta\varepsilon=1\%) = 0.6$, respectively) and plot them on figure 5.

For a good numerical treatment a simultaneous consideration of all the constants is essential. However, in the sequel we deviate slightly from this type of approach in an attempt to give a preliminary guess of dependence of material constants on damage level. The reason for this is that a generally accepted theoretical model of damaged materials of type (1) or (2) does not exist. As approximating functions we tried logarithmic, exponential and power type dependences of the material constants on damage level represented by age time, and cycle ratio as single parameters. Exponential and logarithmic approximations gave rise to very high errors. According to the figure 5, a power type approximation seems reasonable such that:

$$\Psi_h(\tau) = k_1 \tau^{k_2} \quad \text{and} \quad \Psi_h(\nu) = l_1(\Delta\varepsilon) \nu^{l_2(\Delta\varepsilon)}, \quad (15)$$

for previous creep and previous LCF-damage, respectively. It should be noted that due to only four damage levels (including the as-received case as zero-level), an alternative approximation by means of polynomials would permit almost perfect fit. Anyway, we reject such an approximation due to larger number of coefficients appearing in such polynomials.

On the other hand, for both damage types according to decreasing tendency remarked on all the branches at figure 4, and corresponding curves for both previous treatments by LCF we propose here

$$\Psi_\varepsilon = M_1 \exp(-M_2 \varepsilon_P). \quad (16)$$

The same formulae hold also for the other three models. The results of identification are given in the fourth section of this paper.

3 Models Based on Additive Strain as well as Stress Histories

Figures 1.-3. show that all the flow curves are almost parallel. This could be modelled by the so-called Rabotnov's time delay of initial yielding causing either strain or stress accumulation. For a model of additive strain history the following replacements in the equations (7)-(14) is here proposed as follows:

$$\varepsilon_P \Rightarrow \varepsilon_P^{hist} = \varepsilon_P + (E_1 \varepsilon_P + E_2) \Psi_h(h), \quad (17)$$

$$\dot{\varepsilon}_P \Rightarrow \dot{\varepsilon}_P^{hist} = [1 + E_1 \Psi_h(h)] \dot{\varepsilon}_P, \quad (18)$$

where Ψ_h is given by (15) for either of the type of previous damage treatment. The constant E_2 is responsible for a global ("rigid") delay of the flow curve along the abscissa whereas the constant E_1 provides variable delay in the course of straining. In order to make the approach more explicit, let us show all the listed evolution equations with the additive strain history taken into account by means of the above two expressions, i.e. JC, LP, ZH and ZA evolution equations respectively:

$$\sigma = Y [1 + C_1(\varepsilon_P^{hist})^{C_2}] \left\{ 1 + C_3 \ln \left[\frac{\dot{\varepsilon}_P^{hist}}{C_4} \right] \right\}, \quad (19)$$

$$\sigma = Y [1 + L_1(\varepsilon_P^{hist})^{L_2}] \left\{ 1 + L_3 \exp(-L_5 \varepsilon_P^{hist}) \ln \left[\frac{\dot{\varepsilon}_P^{hist}}{L_4} \right] \right\}, \quad (20)$$

$$\sigma = Y [1 + H_1(\varepsilon_P^{hist})^{H_2}] \{ 1 + H_3 \exp(-H_5 \varepsilon_P^{hist}) (\dot{\varepsilon}_P^{hist})^{H_4} \} \quad (21)$$

$$\sigma = Y \{ 1 + A_1(\varepsilon_P^{hist})^{A_2} + A_3(\dot{\varepsilon}_P^{hist})^{A_4} \}. \quad (22)$$

where the dependence of material constants on temperature is suppressed for brevity.

An alternative to the above approach would be to assume an additive stress history by the following stress translation:

$$\sigma \Rightarrow \sigma^{hist} = \sigma - (S_1 \sigma + S_2) \Psi_h(h), \quad (23)$$

using again the representations (15) for the damage history function Ψ_h . To the meaning of the constants S_1 and S_2 might be given similar explanation as in the case of additive strain history. With the above assumption all the listed models are expressed now by means of:

$$\sigma^{hist} = Y (1 + C_1 \varepsilon_P^{C_2}) \left\{ 1 + C_3 \ln \left[\frac{\dot{\varepsilon}_P}{C_4} \right] \right\}, \quad (24)$$

$$\sigma^{hist} = Y (1 + L_1 \varepsilon_P^{L_2}) \left\{ 1 + L_3 \exp(-L_5 \varepsilon_P) \ln \left[\frac{\dot{\varepsilon}_P}{L_4} \right] \right\}, \quad (25)$$

$$\sigma^{hist} = Y (1 + H_1 \varepsilon_P^{H_2}) \left[1 + H_3 \exp(-H_5 \varepsilon_P) \dot{\varepsilon}_P^{H_4} \right] \quad (26)$$

$$\sigma^{hist} = Y (1 + A_1 \varepsilon_P^{A_2} + A_3 \dot{\varepsilon}_P^{A_4}). \quad (27)$$

Of course, values of all the material constants are different for diverse models of histories.

4 Identification of Material Constants

Once the model is chosen, its calibration is far from trivial due to essential non-linearity (i.e. impossibility of its transformation into a linear model) in the space of material constants. The complexity of the problem encountered requires a multi-step procedure. The general approach (explained in detail in [9] for the multi-damage case) is reduced to minimization of the *chi-square function*. In our case this function is the sum of squares of differences of calculated (by one of the above listed constitutive models when model of the damage history is accepted) and experimental stress values over all discrete values of plastic strains and strain rates and for all damage histories. The identification strategy is split into the following two procedures:

4.1 Initial subspace splitting for as-received AISI 316H

A precise initial guess of values for material constants is very important due to the fact that when all the constants of a model are taken into account, then the corresponding *chi-square function* has some singular regions and a lot of local minima leading to erroneous final determination of the material constants. For example, with a wrong initial guess it is possible by a nonlinear best-fit to obtain control strain rates C_4 (JC-model) or L_4 (LP-model) of the order of magnitude $0.1s^{-1}$ which is far from physical reality where such a "static" strain rate should be definitely less than $0.001s^{-1}$ (cf. Tables 1.,2. below where these constants are smaller than $10^{-5}s^{-1}$). For this reason the next approach is very helpful.

In the absence of damage (i.e. for as-received specimens) all the evolution equations (7)-(14) might be represented by the following nonlinear differential equation:

$$F\left(\frac{\sigma}{Y_0}\right) = G_1(\varepsilon_P) + G_2(\varepsilon_P) H(\dot{\varepsilon}_P)$$

where for diverse models the above functions read:

$$\mathbf{JC} : G_1(\varepsilon_P) = \ln(1 + C_1 \varepsilon_P^{C_2}), G_2(\varepsilon_P) = 1, H(\dot{\varepsilon}_P) = \ln \left[1 + C_3 \ln \left(\frac{\dot{\varepsilon}_P}{C_4} \right) \right],$$

$$\mathbf{LP} : G_1(\varepsilon_P) = 1 + L_1 \varepsilon_P^{L_2}, G_2(\varepsilon_P) = L_3 G_1(\varepsilon_P) \exp(-L_5 \varepsilon_P), H(\dot{\varepsilon}_P) = \ln \left(\frac{\dot{\varepsilon}_P}{L_4} \right),$$

$$\mathbf{ZH} : G_1(\varepsilon_P) = 1 + H_1 \varepsilon_P^{H_2}, G_2(\varepsilon_P) = H_3 G_1(\varepsilon_P) \exp(-H_5 \varepsilon_P), H(\dot{\varepsilon}_P) = \dot{\varepsilon}_P^{H_4},$$

$$\mathbf{AZ} : G_1(\varepsilon_P) = 1 + A_1 \varepsilon_P^{A_2}, G_2(\varepsilon_P) = 1, H(\dot{\varepsilon}_P) = A_3 \dot{\varepsilon}_P^{A_4}.$$

whereas the left-hand side stress dependent function reads:

$$\mathbf{JC} : F(\sigma/Y_0) = \ln(\sigma/Y_0),$$

$$\mathbf{LP\&ZH\&AZ} : F(\sigma/Y_0) = \sigma/Y_0.$$

Such a representation allows subsequent development of the functions F, G_1, G_2, H into power series in their arguments and a very precise subsequent determination of initial values of all the material constants for each considered particular model. This procedure has been proposed in [15]. For obvious reason such an approach may be called *initial subspace splitting in the global space of material constants*. When all the coefficients in such polynomialss are determined, then material constants in nonlinear but regular functions F, G_1, G_2, H are determined by some numerical method like Nelder-Mead, Levenberg-Marquardt or some other[10].

In this way values of material constants C_k ($k \in \{1, \dots, 4\}$) (JC-model), L_k ($k \in \{1, \dots, 5\}$) (LP-model), H_k ($k \in \{1, \dots, 5\}$) (ZH-model), A_k ($k \in \{1, \dots, 4\}$) (ZA-model) for as-received specimens are determined. The initial yield stress of AISI 316H in such a virgin state at $550^{\circ}C$ is determined to be:

$$Y_0 = 127.71 \text{ MPa}, \quad (28)$$

for all the material models.

4.2 Final determination of material constants

Following the above proposed procedure the corresponding sets of material constants for all the model histories and evolution equations are obtained. They are given in the following four tables.

The following two diagrams show us the quality of determined material constants for AZ evolution equation at additive stress history representation.

Corresponding diagrams for the other constitutive models do not show any significant discrepancy when compared to figures 6.-7.

JC model	Multi. history	Add. ε -history	Add. σ -history
C_1	$3.305 \pm 6\%$	$4.1317 \pm 9\%$	$2.964 \pm 6\%$
C_2	$0.645 \pm 5\%$	$0.598 \pm 8\%$	$0.624 \pm 8\%$
C_3	$0.019 \pm 5\%$	$0.0011 \pm 10\%$	$0.02 \pm 6\%$
C_4	$6.7 \cdot 10^{-8} \pm 11\%$	$4.9 \cdot 10^{-6} \pm 72\%$	$1.53 \cdot 10^{-8} \pm 17\%$
M_1, E_1, S_1	$1.378 \pm 3\%$	$1.931 \pm 26\%$	$-0.00034 \pm 68\%$
M_2, E_2, S_2	$4.689 \pm 7\%$	$0.932 \pm 3\%$	$1.12 \pm 97\%$
k_1	0.9076	0.2174	1.39
k_2	0.0659	0.0729	0.0646
$l_{1(0.6\%)}$	0.5973	0.1391	0.923
$l_{2(0.6\%)}$	0.0873	0.1049	0.0907
$l_{1(1\%)}$	0.8798	0.2143	1.354
$l_{2(1\%)}$	0.005	0.0107	0.0092
η	0.975	0.9734	0.9744
$\delta\%$	3.06	3.19	3.09

Table 1: Material constants of the Johnson-Cook model based on control strain rate with 99% confidence interval for its material constants

New experiments with damage levels below 0.2 are needed for a better estimation of material constants at such lower damage levels.

The above described numerical approach to the problem of material constants calibration is often underestimated and considered as "a curve fitting exercise" [11]. We, however, find that such an analysis must be correctly performed and exactly explained with explicit confidence characteristics such as correlation coefficient and confidence limits due to the significance of the material constants. In our option the problem of interpreting the data means often terrorizing the experimental data in order to fit them into a doubtful theoretical model based on "microstructural" assumptions. Typically this means extrapolation of some variety of curves to find one material constant, then some other suspicious graphical skill and, finally, a conclusion that the results are satisfactorily precise, without a quantitative statement how precise. Sometimes, as in [8], results of shear and tension are even mutually confused and forced to fit into the same constitutive equation.

LP model	Multi. history	Add. ε_P -history	Add. σ -history
L_1	$5.8 \pm 3\%$	$5.729 \pm 7\%$	$5.692 \pm 2\%$
L_2	$0.855 \pm 1\%$	$0.84 \pm 8\%$	$0.77 \pm 2\%$
L_3	$0.026 \pm 3\%$	$0.0267 \pm 13\%$	$0.034 \pm 2\%$
L_4	$9.4 \cdot 10^{-8} \pm 3\%$	$7.5 \cdot 10^{-7} \pm 22\%$	$2.3 \cdot 10^{-5} \pm 7\%$
L_5	$4.205 \pm 8\%$	$3.5 \pm 17\%$	$7.57 \pm 4\%$
M_1, E_1, S_1	$1.533 \pm 8\%$	$1.092 \pm 41\%$	$-0.00032 \pm 23\%$
M_2, E_2, S_2	$5.7 \pm 2\%$	$0.9845 \pm 3\%$	$1.01 \pm 3\%$
k_1	0.8576	0.2089	1.549
k_2	0.0656	0.0746	0.0575
$l_{1(0.6\%)}$	0.5669	0.1297	1.078
$l_{2(0.6\%)}$	0.085	0.1023	0.0765
$l_{1(1\%)}$	0.8317	0.2019	1.5094
$l_{1(1\%)}$	0.0039	0.0129	0.0082
η	0.9775	0.9735	0.9735
$\delta\%$	2.94	3.09	3.12

Table 2: Material constants of the Ludwik-Prandtl model based on control strain rate with 99% confidence interval for its material constants

ZH model	Multi. history	Add. ε_P -history	Add. σ -history
H_1	$5.229 \pm 4\%$	$4.312 \pm 2\%$	$4.3064 \pm 3\%$
H_2	$0.6396 \pm 3\%$	$0.516 \pm 2\%$	$0.5496 \pm 3\%$
H_3	$0.0398 \pm 28\%$	$0.0065 \pm 42\%$	$0.0242 \pm 34\%$
H_4	$0.3354 \pm 12\%$	$0.466 \pm 13\%$	$0.4165 \pm 12\%$
H_5	$6.55 \pm 11\%$	$3.23 \pm 19\%$	$6.1344 \pm 10\%$
M_1, E_1, S_1	$1.517 \pm 3\%$	$2.59 \pm 11\%$	$-0.0011 \pm 13\%$
M_2, E_2, S_2	$6.91 \pm 3\%$	$0.695 \pm 2\%$	$1.4573 \pm 5\%$
k_1	0.7981	0.2636	1.3475
k_2	0.0683	0.0855	0.0668
$l_{1(0.6\%)}$	0.518	0.1523	0.8837
$l_{2(0.6\%)}$	0.0911	0.1189	0.0951
$l_{1(1\%)}$	0.774	0.2536	1.3149
$l_{1(1\%)}$	0.0045	0.0169	0.0094
η	0.9854	0.9881	0.9874
$\delta\%$	2.36	2.15	2.18

Table 3: Material constants of the Zener-Hollomon model based on control strain rate with 99% confidence interval for its material constants

AZ model	Multi. history	Add. ε_P -history	Add. σ -history
A_1	$4.6296 \pm 3\%$	$4.347 \pm 2\%$	$3.908 \pm 3\%$
A_2	$0.5845 \pm 3\%$	$0.52 \pm 2\%$	$0.5086 \pm 3\%$
A_3	$0.0452 \pm 26\%$	$0.00022 \pm 73\%$	$0.0348 \pm 29\%$
A_4	$0.3394 \pm 11\%$	$1.0826 \pm 10\%$	$0.39 \pm 11\%$
M_1, E_1, S_1	$1.4975 \pm 2\%$	$2.486 \pm 12\%$	$-0.00089 \pm 16\%$
M_2, E_2, S_2	$6.4142 \pm 3\%$	$0.743 \pm 2\%$	$1.376 \pm 5\%$
k_1	0.7617	0.2517	1.3454
k_2	0.0685	0.0826	0.0669
$l_1(0.6\%)$	0.4939	0.1503	0.8819
$l_2(0.6\%)$	0.0916	0.1161	0.0954
$l_1(1\%)$	0.7390	0.2448	1.3129
$l_1(1\%)$	0.0045	0.0143	0.0094
η	0.9861	0.988	0.9877
$\delta\%$	2.28	2.13	2.14

Table 4: Material constants of the Armstrong-Zerilli model based on control strain rate with 99% confidence interval for its material constants

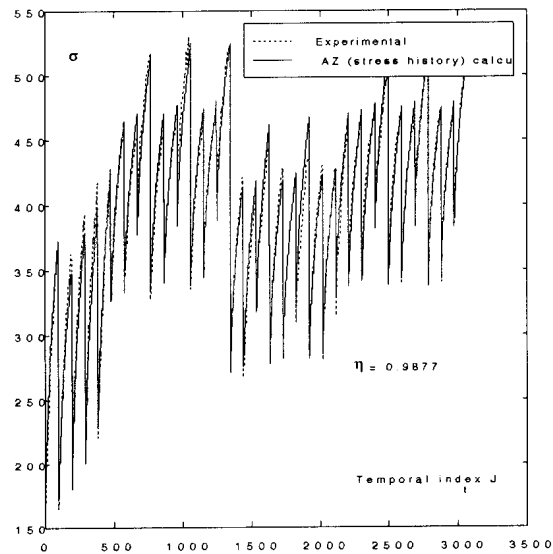


Figure 6: Stresses $\sigma^{\text{exp}}(t)$ and $\sigma^{\text{anal}}(t)$ for additive overstress history influence

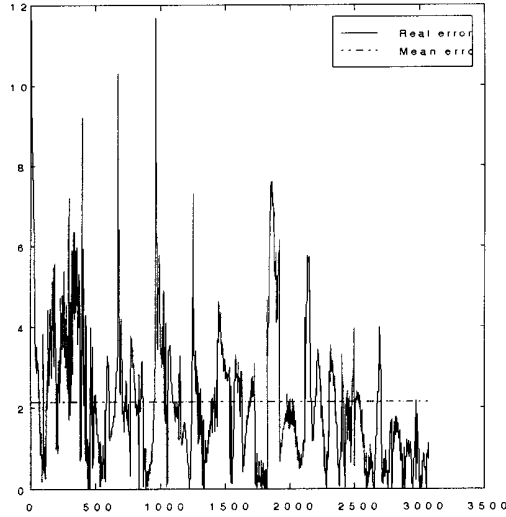


Figure 7: Error $\|\sigma^{\text{exp}}(t) - \sigma^{\text{anal}}(t)\|$ for additive overstress history influence

5 Comparison with Thermal Activation based Models

Another interesting proposal (based on non-linear thermal activation) was made by Klepaczko in [13]. His evolution equation for plastic strain reads:

$$\dot{\varepsilon}_P = \phi(\theta, S_1, S_2, \dots) \exp \left[- \frac{\Delta G(\theta, \sigma, S_1, S_2, \dots)}{\kappa T} \right] \quad (29)$$

where ΔG is the free energy of activation, κ the Boltzmann constant, and S_1, S_2, \dots are scalar internal parameters. If JC-evolution equations without damage history are compared with the above proposal, then we get:

$$\phi = C_4,$$

$$\Delta G = - \frac{\kappa T}{C_3} \left\{ \frac{\sigma}{Y^\# (1 + C_1 \varepsilon_P^{C_2}) [1 - \theta^n]} - 1 \right\}. \quad (30)$$

Similar comparison with LP-model without damage history gives rise to:

$$\phi = L_4,$$

$$\Delta G = - \frac{\kappa T}{L_3} \left\{ \frac{\sigma}{Y [1 + L_1 \varepsilon_P]^{L_2}} - 1 \right\} \exp [L_5 \varepsilon_P]. \quad (31)$$

Consequently, the models with logarithmic presence of plastic strain rate in evolution equation may be transformed to the form originated from the thermal activation approach. The above four formulas allow for a non-linear thermal activation interpretation of the meaning of JC and LP material constants if the damage level is understood as one of the internal parameters. In other words either ε_P could be replaced by ε_P^{hist} for additive strain history approach or σ should be replaced by σ^{hist} for additive stress history approach.

6 Concluding Remarks

The following general conclusions might be drawn for inelastic behaviour of specimens as-received and predamaged by creep as well as by LCF:

- Strain rate hardening is correctly modelled by all the evolution equations since $C_3 > 0$ (AZ-model), $L_3 > 0$ (LP-model), $H_3 > 0$ (ZH-model) and $A_3 > 0$ (AZ-model).
- Damage hardening is also correctly covered by all the constitutive models since for all the models (in all the tables) $M_1 > 0$, $E_2 > 0$ as well as $S_2 > 0$.
- Due to efficient numerical approach agreement between all the models and whole manifold of testing data is obtained. This can be seen from very high correlation coefficients in tables 1.-4..
- A further improvement of history functions in order to unify creep and LCF (cf. (15)) is not advisable because in the case of creep we have to deal with *static strain history* whereas at LCF-prehistory we have a dynamic straining requiring *strain rate history*. An additional restriction is the small number of tests in each of the isolated damage groups for creep, LCF at 0.6% and LCF at 1%.

Concerning the overall material constants for AISI 316H predamaged by creep it can be said that:

- the almost universally applied assumption on additivity of plastic and creep strains has led to extremely low correlation coefficients; thus, previous creep strain has inevitably a non-linear influence on the present plastic strain.
- the initial yield stress is higher then for as-received AISI 316H with a non-linear dependence on creep time, with a curious minimum at the medium creep time, which should be checked by subsequent tests.

For the damage history realized by LCF, the following remark is interesting:

- The increase in LCF strain amplitude causes an increase in the initial yield stress, suggesting that the dependence Y_0/ε_{LCF} might be established treating the as-received case as the special case with $\varepsilon_{LCF} = 0$.

Acknowledgements

Thanks are due to Prof. K. Iida of the Tokyo University for the LCF tests; to Dr. R. Matera of JRC for the creep tests; to Messrs. M. Forlani and A. Pachera of JRC for the dynamic tests; to Prof. G. Milovanović of the University of Nis for discussions concerning the numerical modelling of data; and to Mr. D. Veljkovic of Kragujevac University for making programming and numerical calculations.

References

- [1] Iida K. , Yoshie S. , Albertini C. , Montagnani M. : *Impact properties of AISI 316H fatigued in LCF*. In : **2nd Int. Conf. on LCF**, Munich: VDM 1973.
- [2] Albertini C. , Montagnani M. : *Dynamic material properties of several steels for fast breeder safety analysis*. **Report EUR 5787 EN** (1977).
- [3] Albertini C. , Eleiche A. M. , Montagnani M. : *Instabilities at high strain rate of AISI 316H damaged by creep, fatigue and irradiation. Discussion of adiabatic temperature oscillations*. **Inst. Phys. Conf. Ser.** 102/10 (1989) pp.503-510.
- [4] Perzyna P. : *Temperature and rate dependent theory of plasticity of crystalline solids*. **Rev. Phys. Applique**, 23 (1988) pp.445-459.
- [5] Cernocky E. P., Krempl E. : *A theory of thermoviscoplasticity based on infinitesimal total strain*. **Int. J. Solids Structures**, 16 (1980) pp.723-741.
- [6] Mićunović M., *A thermodynamic model of ideal cyclic viscoplasticity*. **Transactions of SMIRT-9**, L. Wittmann, F. H. (ed.) Rotterdam: Balkema 1987, pp.195-203.
- [7] El-Magd E., Hellwing K. J., Hock H. G., Homayun M. : *Mechanical behaviour of austenitic steel and aluminium with respect to elastic- plastic wave propagation*. **Mat. Techn.-Steel Res.**, 58/1 (1987) pp.33-39.
- [8] Johnson G. R., Cook W. H. : *A constitutive model and data for metals subjected to large strains, high strain rates and high temperatures*. **7th Int. Symp. on Ballistics**, P4.5, The Hague 1983, pp.541-547.
- [9] Montagnani M., Albertini C., Mićunović M.: *Uniaxial viscoplastic experiments of predamaged AISI 316H*, in: **CREEP IN STRUCTURES** (ed. M. Zyczkowski), **IUTAM Symposium Cracow/Poland 1990**, pp. 401-408, Springer Verlag.
- [10] Press W.H., Flannery B.P., Teukolsky S.A., Vetterling W.T.: **NUMERICAL RECIPES - THE ART OF SCIENTIFIC COMPUTING**, Cambridge University Press 1986.

- [11] Harding J.: *The development of constitutive relationships for material behaviour at high rates of strain*. **Inst.Phys.Conf.Ser.** 102/5 (1989) pp. 189-203.
- [12] Zerilli F.J., Armstrong R.W.: *Dislocation-mechanics-based constitutive relations for material dynamics calculations*, **J.Appl.Phys.**, 61/5 (1987) pp. 1816-1825.
- [13] Klepaczko J.R.: *Constitutive modelling in dynamic plasticity based on physical state variables - a review*, **J. de Physique**, C3/49 (1988) pp. 553-560.
- [14] Mićunović M.: *Inelastic memory versus viscoplasticity of continuously damaged materials*. **J.Mech.BehaviorMater.**, Vol. 4.,No.4., (1993) pp. 331-341.
- [15] Radosavljević M.: *A stochastic modelling of experimental data*. **YUMEH'97 (Yugoslav Conf.Mech.)**, Vrnjacka Banja (1997) pp. 331-341.

VISKOPLASTIČNO PONAŠANJE ZAMORENOG ČELIKA AISI 316H IZ DINAMIČKIH EKSPERIMENATA

M. Mićunović, M. Radosavljević, C. Albertini, M. Montagnani

Dve grupe uzoraka prethodno izloženih puzanju ili niskocikličnom zamoru su ispitane zatezanjem na temperaturi od 550⁰C u širokom opsegu brzina deformacije [10⁻³, 10³] s⁻¹. Epruvete su prethodno izložene ili puzanju pri različitim vremenima puzanja ili niskocikličnom zamoru sa različitim deformacionim amplitudama i različitim brojevima deformacionih ciklusa. Evolucionarne jednačine su kalibrisane za devičanski, prethodno puzajući i prethodno niskociklično zamoren materijal. Materijalne konstante koje se u ovim jednačinama pojavljuju zavise od istorije i nivoa zamora. Upoređenja sa nekim empiričkim i mikrostrukturnim modelima su izvedena.